EUROPEAN JOURNAL OF BIOMEDICAL AND PHARMACEUTICAL SCIENCES
http://www.ejbps.com

ISSN 2349-8870
Volume: 4
Issue: 8
587-602
Year: 2017

A FUNCTIONAL INJECTABLE HYDROGEL FOR NUCLEUS PULPOSUS REGENERATION IN LAPINE INTERVERTEBRAL DISC DEFECT MODEL

Mir Mahmoud Mortazavi R.*[1], Suresh Babu S., Harikrishnan V.S. and Annie John[2]

[1]Biomedical Technology Wing, Sree Chitra Tirunal Institute For Medical Sciences and Technology, Trivandrum 695012, India.
[2]Advanced Centre for Tissue Engineering, Dept. of Biochemistry, University of Kerala, Thiruvananthapuram – 695 581, Kerala, India.

***Corresponding Author: Dr. Annie John**
Advanced Centre for Tissue Engineering, Dept. of Biochemistry, University of Kerala, Thiruvananthapuram – 695 581, Kerala, India.

Article Received on 02/06/2017 **Article Revised on 23/06/2017** **Article Accepted on 13/07/2017**

ABSTRACT
Nucleolus Pulposus (NP) of the Intervertebral disc (IVD) is the first tissue to initiate degeneration especailly from a younger age which eventually leads to low back pain. IVD degeneration happens due to unusual sitting, trauma, genetic inheritance and impaired nutrient exchange between nucleus pulposus and blood vessels. If the extracellular matrix of NP remains the same throughout life, the disc height will not collapse. In this study, alginate was selected as the material of choice to mimic the NP. Alginate hydrogel was made in different concentrations incorporating strontium and tested for the required compression strength to mimic the real NP which is always under constant pressure. The designed and fabricated Alg/Sr hydrogel was tested for cytotoxicity to depict the safety of the material and further tested *in-vitro* by mimicking an *in vivo* 3 dimensional structure incorporating cells which was ultimately injected *in situ* at the physically damaged NP site of the lumbar vertebrae (L3-L4/L5-L6) of New Zealand White rabbits *in situ.* This study showed that Alg/Sr Hydrogel is permissive and a promising hydrogel which can encapsulate cells for secreting extra cellular matrix (ECM) to restore the collapsed disc height to a certain extent to enable temporary relief of low back pain.

KEYWORDS: Nucleus pulposus, Alginate/Strontium Hydrogel, Intervertebral Disc Lapine IVD model.

INTRODUCTION
In the first year of life, NP cells as well as notochordal cells are abundant to enhance secretion of extra cellular matrix like proteoglycans and aggrecans. They make a rich fiber network with different ions including Na^+ and K^+ and are responsible for fluid absorption towards the central region of NP. This rich environment act like a semipermeable membrane to absorb water from the surrounding tissue.[1] More the water absorption, greater is the increase in the disc height. Degeneration of intervertebral disc may occur in the nucleus pulposus (NP) especially from childhood. After the disappearance of notochordal cells from NP in the first year of life, from NP, the chondrocyte cells are the only cells at the center of NP which can continue enriching the extra cellular matrix by secreting collagen fibers.

As age steps in, NP looses stamina; proteoglycans and aggrecans get fragmented by different types of matrix metalloproteinase (MMPs).[2] Long chains of proteoglycans and aggrecans get shorter and shorter. They lose the properties of acting like a semipermeable membrane. By decreasing the density of Na^+ and K^+ ions, disc looses water content and disc height will collapse[3], resulting in disc bulging and herniation. There are different grades of disc herniation which leads to severe surgery like total disc replacement or partial disc replacement.[4] Herniation of intervertebral disc (IVD) leads the vertebral column to different types of deformities like scoliosis, spondylolisthesis, kyphosis and lordosis.[5] In the US, back pain is the most expensive treatment where the overall cost for treatment is around $ 91 billion per year.[6],[7] Over 80% of the younger generation below 45 years old complains of back pain which is related to less activity of their body.[7]

Tissue engineering technique can be applied for the regeneration of the damaged intervertebral disc before it reaches a severe condition,[8],[9] There is a tremendous surge to use natural biomaterials for regeneration and repair.[10],[11] One of the natural biomaterials is alginate[12],[13] suitable for such applications.

Alginate is extracted from large marine brown alga like Laminaria hyperborean - a hydrophilic polysaccharide that give stamina to brown algae. They are present in the cell wall and intercellular matrix providing the strength and flexibility to withstand the force of water.[10]

Alginate can be designed as an injectable hydrogel for NP repair[14],[15] and is the trusted natural bio scaffold which has served in different applications like delivery vehicles for drugs, cell encapsulation and mimicking extracellular matrix.[16] Properties of alginate can be modified for several applications by adjusting the percentage of the component to entice cell attachment, strength, mechanical stiffness, swelling and binding or release of bioactive molecules in coherence with the nature of the properties of the target tissue[13], [17],[19]

MATERIALS AND METHODS

Fabrication of Alg/Sr Scaffold in different combinations and characterizations

Alginate - strontium hydrogel was prepared *via* dripping of 4 percentage of alginate solution in different concentration of strontium solution (1,1.2,1.4,1.6,1.8 and 2%). All solutions such as alginate and strontium chloride for the fabrication of Alg/Sr hydrogel were previously prepared using 0.22µm sterile syringe filter. Alg/Sr Hydrogel was prepared in two forms - Alg/Sr Beads as well as Alg/Sr Gel for *in vitro* cytotoxicity and 3D cell culture evaluations (fig 1).

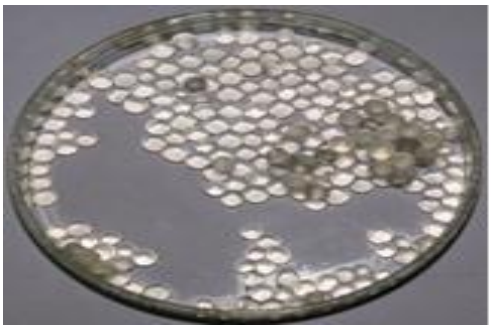

Fig 1: Visible Alg/Sr Beads in petri dish.

Chemistry of Alginate and Strontium

Strontium is available in nature - soil, water, plants and animals. Measure of Sr in soil varies from 0.001 to 39mg/l. In the normal diet of drinking water there is 2-4 mg of Sr per day and available in vegetables.[20] The other substance is Alginate which belongs to an important family of hydrophilic unbranched, linear polysaccharide found in seaweed and bacteria. It is made of two types of monosaccharides (Mannuronic acid, Guluronic acid) and very suitable for different types of hydrogel matrix (fig 2).[21] Efficiency of alginate for preparing hydrogel with different compositions and mechanical properties made this polysaccharide a suitable natural biomaterial for cell encapsulation to control the release of macro molecules, proteins and nucleic acid.[10] Alginate and glycosaminoglycans have negative charges. Taking advantage of the dual properties, a combination of Alg/Sr Hydrogel was prepared to enable easy handling and injection into the intervertebral disc. Simultaneously, the ionic and covalent linkages of strontium could help the gelation of alginate (fig 1).[22] Divalent cations like strontium also bind to the G-blocks in the Alg/Sr hydrogel.[23]

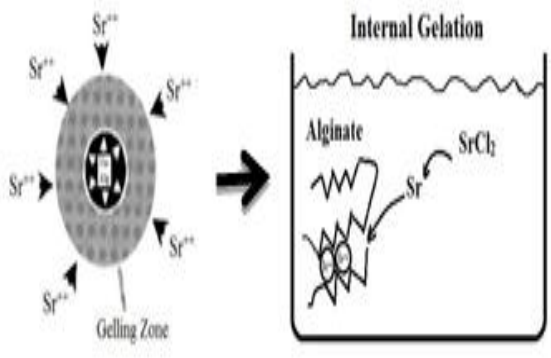

Fig 2: Chemistry of material synthesis of alginate-strontium hydrogel

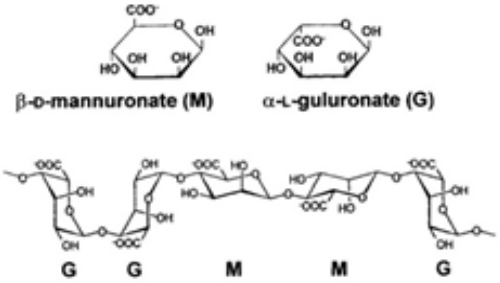

Fig 3: Schematic structure of alginate monomers.

Compression test

Compression was measured using the INSTRON machine (INSTRON Model 3345, force transducer: Model 2519_107, Capacity 5000N, S/N 64512) for the tolerance of Alg/Sr gel against the load. Each Alg/Sr hydrogel bead was examined in the same machine and placed in the acrylic mold for compression test. Force transducer speed was adjusted 0.5 mm per minute and speed resistance of Alg/Sr hydrogel was measured.

POROSITY OF ALG/SR HYDROGEL

Three-dimensional micro-computed tomography analysis to detect Porosity

Alg/Sr hydrogel was analyzed using a desktop µCT (µCT 40, Scanco Medical AG, Brüttisellen, Switzerland) at 45 kVp and 114µA x-ray tube energy 6µm voxel size and 0.2 second integration time with approximately 30 slices per specimen. The 3D stained hydrogel with osmium tetroxide was scanned and data determined by the µCT software. Hydrogel sample was prepared by lyophilizing for 24 Hours and stained with osmium tetroxide to enhance the contrast. Again sample was lyophilized for 24 hours and scanned with desktop µCT.

Scanning Electron Microscopy

Lyophilized Alg/Sr hydrogel stained with osmium tetroxide for enhancing contrast of hydrogel during imaging, was coated Gold-Palladium (Au-Pd) in an ion sputter (Hitachi E-1010) and viewed under the Scanning Electron Microscope (Hitachi S2400) to observe the 3D porous structure.

Histology
Cryosections of frozen Alg/Sr lyophilized hydrogel samples were taken in the Cryostat (Leica CM 3050S) and stained with H & E, to visualize the internal morphology and porous structure.

Radiographic analysis on the opacity of the hydrogel
Prior to implantation, the clinical X ray of the hydrogel scaffold was taken for evaluating radiopacity by using X-Ray Equipment (SIEMENS, Model: 3135071) to determine the radiopacity of Alginate Strontium hydrogel and hydroxyapatite (ceramic) was taken as the reference material.

Thermogravimetry (TGA)
TGA determined the thermal stability and compositional analysis of the sample on a SDT Q600, (TA Instruments Inc., USA). Periodic calibration of temperature and mass signals of the DSDT Q600 was done using standard reference hydrogel. The test method is based on ASTM E 1131-08.

Fourier Transform Infrared Spectroscopy (FTIR)
FTIR measurement was done by using Thermo Nicolet (Madison, WI) 5700 spectrometer (USA) and widespread spectra gathered together in the diffuse reflectance (DRIFT) mode. FTIR was done on the powdered lyophilized of Alg/Sr hydrogel as sample and Alginate alone as control.

IN VITRO TESTS
Cytotoxicity studies
Direct contact method for Cytotoxicity was performed for hydrogel. Samples in triplicate were placed on sub confluent monolayer of L-929 mouse fibroblasts Cell Line. After incubation of cells at 37± 1˚C for 24 ± 1 h, cell monolayer was examined for cellular response around the hydrogel samples using Phase Contrast Microscope (Leica DMI 6000). The reactivity was graded as 0,1,2,3 and 4 based on zone of lysis, vacuolization and detachment.

Animal ethics and stem cell approval
MSCs have been approved by the Institutional Committee for Stem Cell Research and Therapy (IC-SCRT: SCT/IC-SCTY/11/JAN 2013). Animal experiments were performed following the guidelines and recommendations of the Committee for the Purpose of Control and Supervision of Experiments on Animals, India (CPCSEA) and with the approval from Institutional Animal Ethics Committee (IAEC: B3112010VIII). ADMSCs were isolated from the subcutaneous adipose site of New Zealand white rabbits weighing around 2–2.5 kg. With the animal under anaesthesia, subcutaneous fat of approximately 5g was isolated and collected in PBS with antibiotics.

Cell culture and cell growth in Alg/Sr hydrogel
Adipose tissue was washed intensively with phosphate-buffered saline (PBS) thrice, minced thoroughly and treated with 1% type I collagenase (Sigma Aldrich, St. Louis, MO) at 37˚C. Enzyme activity was neutralized with a minimal essential medium (a-MEM) containing 10% fetal bovine serum (FBS), 200Uml-1 of penicillin and 200Uml-1 of streptomycin (double dose) (Gibco, India). The solution was then centrifuged at 1200g for 10min. The pellet was filtered by 180µm nylon mesh to remove cellular debris and was plated in a 25 cm^2 flask (Nunc, India) containing 5 ml of medium with a single dose of antibiotics and incubated in 5% CO_2 at 37˚C in humid atmosphere.

Following incubation, the medium was changed after 24hours to remove residual non adherent red blood cells. The primary cells were cultured for 4-5 days until they reached confluence and were defined as 'Passage 0'. After 5 days in primary culture, the adherent ADMSCs were released with 0.25% trypsin–EDTA (Gibco, India) and centrifuged at 2000 rpm for 10min and subcultured for subsequent passages until 'Passage 3' and cells were characterized prior to experiments. The morphology of the confluent fibroblast-like cells was viewed under the phase contrast microscope.

Cell surface characterization
RADMSCs (1 x 10^5 cells - Passage 4) were cultured in 25 cm^2 flask (Nunc) for 48h at 37˚C in a humid atmosphere and 5% CO_2; washed with PBS; trypsinized with 0.25% trypsin-EDTA for 5min and centrifuged at 300g for 10min. The pellet was blocked with 3% BSA (50µl) in PBS for 30 min and further incubated in PBS containing 1µl monoclonal antibodies (FITC labeled, BD Biosciences, USA) to CD 90 and CD 105 at 4˚C for 1h. The intensity of fluorescence was recorded under flow cytometry (BD Biosciences, FACS Aria). RADMSCs without staining, but trypsinized, fixed and washed under the same conditions were used as the control. 10^4 or 10,000 cells were counted in the hemocytometer chamber. Parallely, cell counting was 1.2e+05, verified using a Scepter Cell Counter.

Fabrication of 3D tissue-engineered construct -Cell titer test
Alg/Sr Hydrogel was plated in 48 wells plate with RADMSCs (passage 4) trypsinized with 0.25% trypsin-EDTA for 5 min and centrifuged at 300g for 10min. The pellet was resuspended in 1 ml medium and the cell number was counted manually using hemocytometer as well as Scepter Cell Counter. 1×10^6 cells/cm^2 were seeded on Alg/Sr Hydrogel in each well.

Encapsulation of MSCs in 3D cylindrical gel block
RADMSCs $1.2*10^5$ were encapsulated in 3 D cylindrical Alg/Sr hydrogel blocks 5mm for mimicking *in vivo* condition. Cells in Hydrogel block were observed and photographed by Light Microscope DM 6000.

Actin staining
Combination of Alg/Sr with encapsulated RADMSCs ($1x10^5$ cells-Passage 4) were cultured for 48 h at 37˚C in

a humid atmosphere and 5% CO_2 on glass cover slips (Blue star India) and thereafter washed with PBS and fixed with 3.7% paraformaldehyde in Sorensen phosphate buffer. The cells washed with PBS were permeabilised using 0.1% Triton X-100 (Sigma) for 5min in PBS. After washing thrice with PBS, the cells were stained with FITC actin (Sigma) 1: 1000 in PBS) for 30min and DAPI (D9564 – Sigma) for 1 h (1: 500 in PBS) in dark at room temperature for determining actin filament (green) and nucleus (blue). The cells were then washed thoroughly with PBS and observed under fluorescent microscope (Nikon Eclipse E600).

Cell viability assay

Rabbit adipose derived cells (1 x 10^5 cells) were seeded into the Alg/Sr hydrogel and placed in 96 wells TCPS plates (Nunc). After being incubated at 37°C, adhered cells were maintained in MEM with 10% FBS, 100units/ml of penicillin and 100µg/ml streptomycin and incubated at 37°C in humid atmosphere and 5% CO_2. MSCs encapsulated within Alg-Sr hydrogel placed on glass cover slips (Blue star India) were washed with PBS and fixed with 3.7% paraformaldehyde in Sorensen phosphate buffer. The cells washed with PBS were permeabilised using 0.1% Triton X-100 (Sigma) for 5min in PBS. After washing thrice with PBS, the cells were stained with acridine Orange (1: 1000 in PBS) for 30min and ethidium bromide 1 h (1: 500 in PBS) in dark at room temperature for determining Acridine Orange (Green- live cell stain) and ethidium bromide (Red- dead cell stain). The cells were then washed thoroughly with PBS and observed under fluorescent microscope (Nikon Eclipse E600).

In vivo Experiments - Rabbit Intervertebral disc (IVD) defect model

To study the real situation of the intervertebral disc regeneration *via* the tissue construct product, an *in vivo* experiment was performed to reveal the effect of treatment on cartilage tissue repair**.** So in this study New Zealand White rabbits lumbar discs (n=30; age = 8-12 month; L3-L4/L4-L5) were selected for testing Alg/Sr hydrogel[24] to compare the regeneration capacity of bare hydrogel with hydrogel encapsulated cells.

Rabbit Implantation experiment

In vivo studies with Rabbit IVD model development and implantation were performed following the guidelines and recommendations of the Committee for the Purpose of Control and Supervision of Experiments on Animals, India (CPCSEA) and with the approval from Institutional Animal Ethics Committee (IAEC) (IAEC: B3112010VIII). Execution, evaluation and reporting of animal experiments were as ARRIVE Guidelines.

Thirty adult rabbits with an average body weight of 2-2.5kg were used. Experimental animals were divided into four groups. All rabbits except positive control animals, passed one month degeneration period to develop IVD rabbit model. Experimental groups were defined for different period of study - 1, 3 and 6 months. Numbers of defects were one or two per animal.

Development of Rabbit IVD Model and Resurgery

The rabbits were anesthetized with intramuscular injections of ketamine@50mg/Kg and xylazine @5mg/ Kg. After the animals lost pinna pinching reflex, the hair over the surgical field was shaved. The rabbits were placed in a lateral decubitus position with an approximate 20 degrees inclination provided by a folded cloth towel placed longitudinally under the animal. Aseptic technique was used for all surgical procedures. The surgical field was disinfected with povidone iodine solution and draped. A posterolateral retroperitoneal approach was used to expose the IVD. A longitudinal skin incision was made from the inferior margin of the rib cage to the pelvic rim, about 2cm ventral to the paraspinal musculature. The left anterolateral vertebral column from L1-L7 was exposed by sharp and blunt dissection of the overlying subcutaneous tissue, retroperitoneal fat, and musculatures.

Disc levels were identified using the pelvic rim as an anatomic landmark for the L5-L6 disc level. One of the lumbar IVD L4-L5 or L5/L6 was punctured by a 16-gauge needle to a depth of about 4mm in the left anterolateral annulus fibrosus. The depth of penetration was controlled by a locking forceps clamped 4mm from the needle tip. Proper and adequate precaution was ascertained by viewing the out flow of gel like nucleus pulposus. The muscles were opposed with non-absorbable 3-0 braided silk sutures in a continuous lock-stitch pattern, while a non-absorbable 3-0 braided silk suture was used to close the skin incisions in a simple interrupted pattern. All animals were monitored until they regained consciousness. The rabbits were allowed to eat and drink, while their healing status was monitored on a daily basis. All animals continued to receive pain medication with meloxicam@0.2mg/kg once daily and Ampicillin-Cloxacillin injection@10mg/Kg twice daily for seven postoperative days.

Radiography

Radiographs were taken after administration of xylazine and ketamine hydrochloride @5mg/kg and 50mg/Kg intramuscularly. To obtain similar degrees of muscle relaxation each time, which may affect the disc height, a consistent level of anesthesia was monitored during radiographic imaging of each animal and at each time. Post IVD injury one month is the Rabbit IVD model.

Re-surgery and injection of bare Alg-Sr hydrogel/cell combination

Re-surgery to inject the bare Alg-Sr hydrogel/cell combination using the dual applicator with a 22 gauge needle was carried out after approximately 30days after the first surgery and radiographic confirmation of the planned IVD damage. Approach and methodology of anesthetic regimen, aseptic precautions, surgical approach as well as post-operative analgesia and care

was similar to the initial procedure mentioned above. Radiograph which confirmed the IVD damage was used to locate the damaged IVDs while the approach to the damaged IVD site was through the right side during re-surgery. The other side was chosen since the healing process might alter the tissue anatomy due to adhesions and might not render proper vision and easy access for the healing injections.

Rabbit gait and behavior–post surgery and post implantation

Rabbit behavior and movement were checked pre and post-surgery of IVD model as well as before and after re-surgery. (IVD degenerative model is created, the rabbit should be able to walk and stand after surgery. This showed that puncturing has just damaged the intervertebral disc and there is no damage to the spinal cord and Rabbit gait and behavior appeared normal) take it to results.

Post implanted evaluations in Rabbit IVD model

Post implanted one month degenerative IVD rabbit model was evaluated by X-ray and MRI (T2 MRI method) and histology of injured and post implanted lumbar vertebrae of all study groups by light microscopy. Further, post implanted IVD was evaluated for disc grading remarks based on histomorphotometry measurement and Disc Height Index.

Histological evaluation

The retrieved IVD post implanted, sham and control tissues after fixing in 10% neutral buffered formalin underwent dehydration in ascending series of isopropyl alcohol followed by infiltration in methyl methacrylate (MMA). Infiltered samples were then embedded in MMA containing 1% Benzoyl peroxide under vacuum. Thin plastic sections (120-140 microns) were sectioned from the PMMA embedded blocks using high-speed precision saw (Isomet TM 2000, Buehler, USA) and polished down manually to 70–90 microns using variable speed grinder polisher (Eco met 3000, Buehler, USA). PMMA embedded polished sections were stained with Hematoxylin and eosin and viewed under the Light microscope (Leica DM 6000).

Histomorphometric evaluation

The Hematoxylin and eosin stained sections were scanned for measuring the percentage of newly regenerated IVD. 1.25x, 5x and 50x magnification were selected randomly and sections were photographed with a CCD camera. These images were suitably calibrated using an inbuilt image configuration. The area of newly regenerated IVD "yellowish colour" was measured using the Quips programme of Q Win software of the microscope (Leica DM 6000). The percentage of newly formed IVD was calculated with respect to the total frame area in the image (μm^2).The percentage of material degraded was calculated by assuming that the total frame area was occupied completely with the newly regenerated NP.

Disc Grading Evaluation

Disc grading remarks were done on the basis of regeneration and disc height of sham, bare hydrogel and hydrogel with cells Rabbit Groups compared to the positive control rabbits.

RESULTS AND DISCUSSION

In this study New Zealand White rabbits have been used due to easy handling and less food consumption.[25],[26] Rabbit lumbar vertebrae were selected as part of interest for IVD research. Intervertebral disc was separated from vertebral column and cleaned from extra muscles. White area amidst vertebrae bone appeared as the location of the intervertebral disc. Location of the intervertebral disc was determined by using X-Ray imaging. After sectioning of each vertebrae, IVDs with jelly center were visible. Nucleus pulposus dried after 60 minutes at room temperature due to their jelly structure.[27]

Compression test

Alginate and strontium solution were prepared in several concentration. Finally the optimum concentration for alginate characterized on 4% passed through 22 G needle for injection in the central region of intervertebral disc. Strontium solution was adjusted in 3 different concentrations 1.2%, 1.8% and 2% (Material 1, 2, & 3 - Fig 4). Compression test of Alg/Sr Hydrogel indicated that 1.8% of Sr incorporated with Alginate gave good strength compared to 1.2% of Sr. Material 3(2% of Sr) gave a strength which is very high compared to Material 1 and 2. It is not suitable for injecting application due to the blockage through 22G needle. Among different types of hydrogels, combination of Alginate and strontium gave better properties to hydrogel for load bearing and cell encapsulation. Other developed hydrogels like chitosan–poly (hydroxybutyrate-co-valerate) with chondroitin sulfate[28], PLLA/alginate[29], Type II collagen-hyaluronan[30] and methacrylated gellan gum (GG-MA)[31] did not favour *in-vivo* regeneration. Alg/Sr hydrogel (M2) showed high resistance around 0.18mPa stiffness like NP, easily passing through 22 G needle. This combination of material M2 was the best option among the other two hydrogels. M3 was not passing through 22G needle while stiffness was very high and M1 was passing easily through 22G needle but stiffness was very low. In the comparison test displacement, M2 and M3 was almost similar to each other.

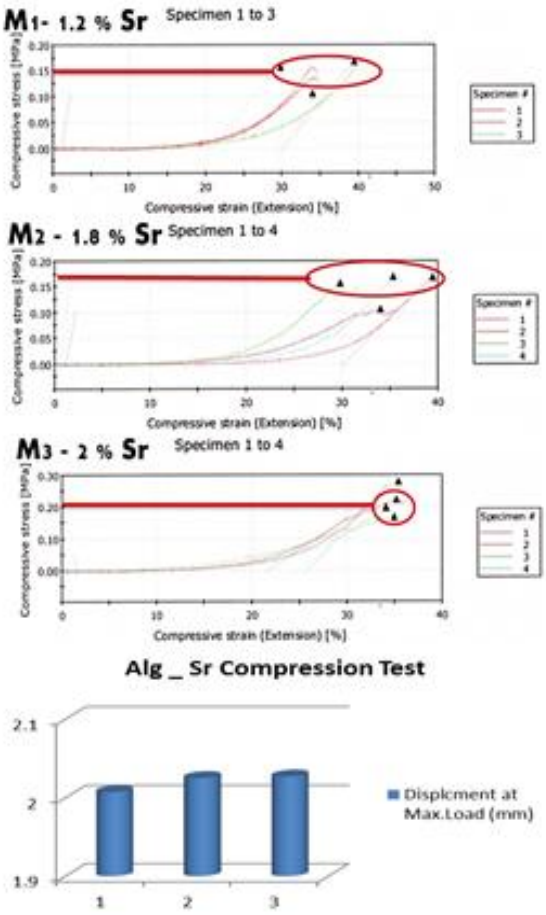

Fig 4: Compression test of Alg/Sr hydrogel estimated by INSTRON machine. M3 shows displacement at Max. load (mm)

Porosity of Alg/Sr hydrogel

Three-dimensional micro-computed tomography analysis to detect Porosity

Mechanical properties, porosity and cell encapsulation were the main parameters aimed of designing this type of hydrogel which can be injectable with an applicator to form the hydrogel directly in the *in-situ* condition. Alginate mimicking the nucleus pulposus provides a niche for cells to encapsulate within the gel. Strontium played a big role as an oxidizing agent in this hydrogel and provided covalent and ionic bonds with alginate monomers (Sakai et al., 2008; Suguna and Sekar, 2011).

µCT revealed a 3D structure of 1.8% Alg/Sr hydrogel block with a porosity of 74.28%. Three dimensional hydrogel block stained with osmium tetroxide enhanced the contrast of the infra-structure of the hydrogel block. Nucleus Pulposus contains 75% of water content and 25% of other ingredients like proteoglycans and collagens (Colombini et al., 2008; Iatridis et al., 2007; Shankar et al., 2009). This porosity is optimum for NP repair (Dadsetan et al., 2008) and mimics the structure of NP. Images of µCT indicate inter connectivity of pores in the hydrogel block with thick walls. The pore distribution (visible in green color) encourages cell migration and attachment to the walls of the hydrogel block.

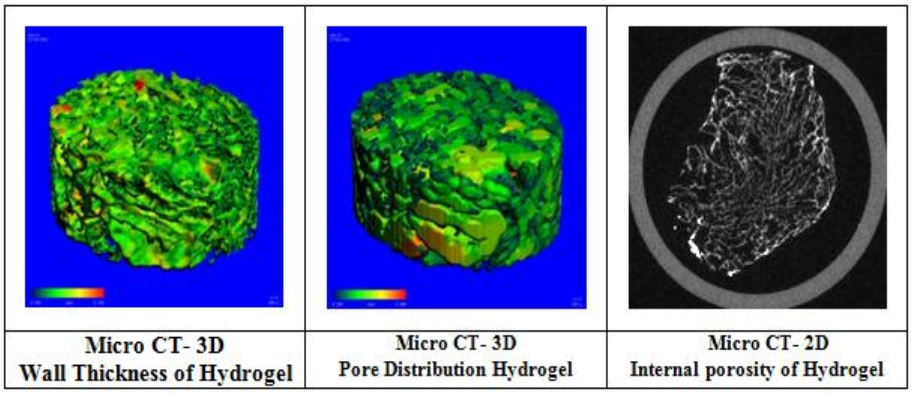

Fig 5: µCT of Alg/Sr Hydrogel Block indicates internal porosity of 1.8% of Alg/Sr Hydrogel.

Scanning Electron Microscopy

There were two forms of hydrogel constructs with 16 G needle and 22 G needle assessed by SEM analysis. Hydrogel with 22 G needle had more porosity compared to 16 G needle. Therefore thickness of the applicator needle has direct effect on the porosity of the hydrogel. When the needle is thinner, porosity of hydrogel will be more. But these techniques have their own barriers.

Designed hydrogel should be able to pass through the desired needle which should not injure the annulus fibrosus of the intervertebral disc during material injection.

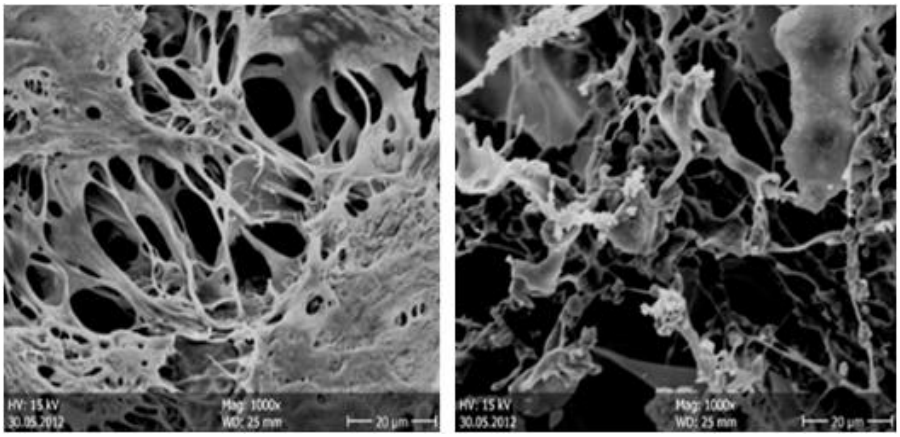

Fig 6: Scanning Electron Micrographs of 16 G and 22 G needle Hydrogel. (Mag. 1000X).

Histology

Alg/Sr hydrogel has been cryosectioned to ensure the porosity under normal condition. Toluidine blue stain was used for each section. There was visible porosity overall each section. 1.8% Alg/Sr Hydrogel beads revealed an elaborate interconnected porous network structure. The niches allow cell migration and adherence to different parts of hydrogel.

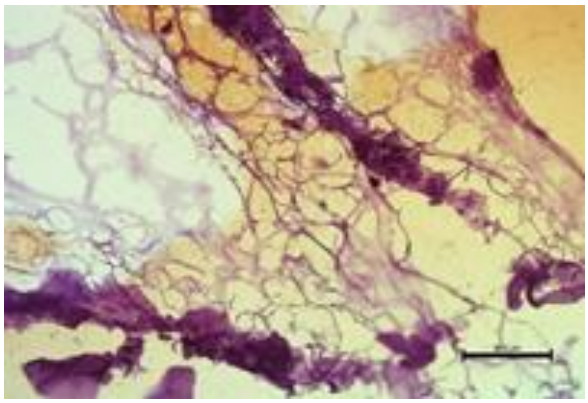

Fig 7: Light Micrograph of cryosectioned toluidine blue stained Alg-Sr hydrogel beads depicting the porous network (Mag. 10X).

Radiographic analysis on the opacity of the hydrogel

Radiography of Alg/Sr hydrogel revealed some other fact regarding this hydrogel. Alg/Sr hydrogel is capable to be traced under the X-ray beam due to radiopacity. Tracking of hydrogel was enabled due to the presence of strontium in the hydrogel beads. Hydroxyapatite has been radiographed as the reference material. Radiograph properties of strontium reveal alginate bead even in low percentage compared to hydroxyapatite material (Lam et al., 2015).

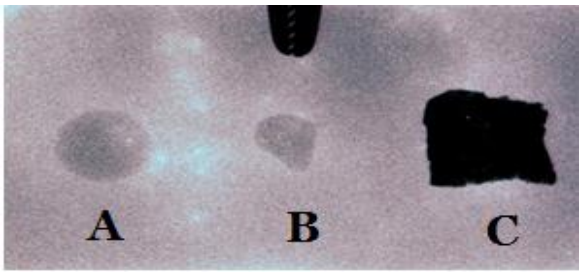

Fig 8: Radiopacity of Alg/Sr beads in X-ray Radiographs (A, B). Hydroxyapatite material (C).

Differential thermal analysis (DTA)

Researchers are trying to investigate any material under different conditions. Three dimensional hydrogel network include ionic and covalent bonding. By increasing the heat of the hydrogel, fluid is released and later on water is absorbed from the surrounding tissue. Thermally reversible hydrogel are not only interesting but important for commercial purpose.[32] [33] An enthalpic change does not occur by heat on this hydrogel. The graph showed structural changes at 66.2 ^{0}C which was reverted to the main structure after 70^{0}C.

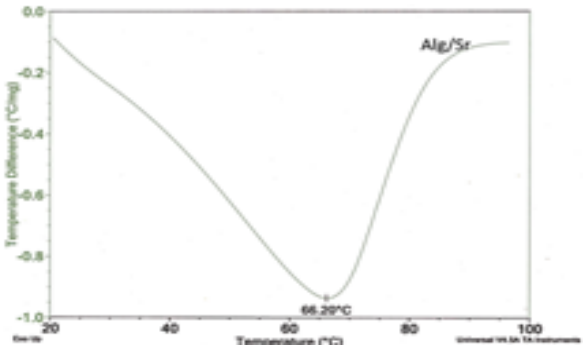

Fig 9: Enthalpic changes and temperatures at which these events occur.

Thermogravimetry (TGA)

Further investigation of thermogravimetric analysis of Alg/Sr hydrogel indicated that material mass loss is 87%

at 37^{0}C. It means that by reaching 37^0 C which is like the human body, material water loss is just 13% and still 87% of material is remaining at that temperature. By increasing the temperature in the open area, the rest of the hydrogel water will vapor at the 79.01^{0}C.

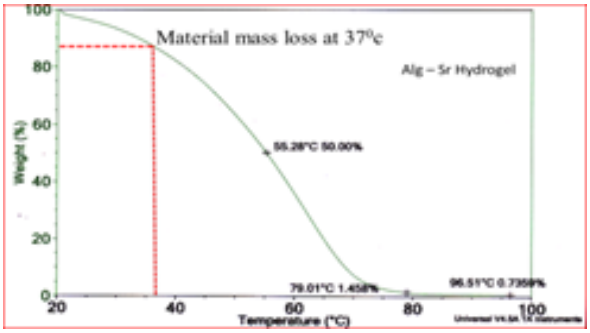

Fig 10: Mass loss of total weight of Alg/Sr Hydrogel.

Fourier Transform Infrared Spectroscopy (FTIR)

Component of this hydrogel was tested by fourier transform infrared spectroscopy (FTIR). Alginate peaks were similar to Alg/Sr hydrogel due to the ionic and covalent bond in hydrogel.

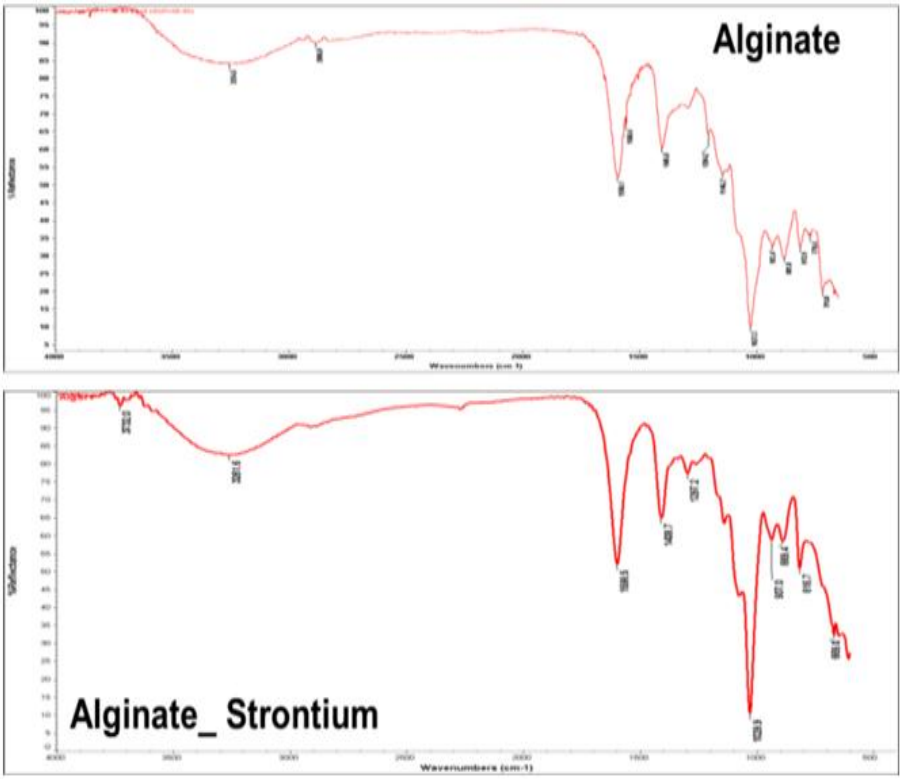

Fig 11: FTIR Spectra of Alginate powder and Alg/Sr Hydrogel.

***In Vitro* analysis of Alg/Sr Hydrogel**

Cytotoxicity studies

Before initiation of *in vivo* experiments, any material should be biocompatible to be used safe in the human body.[34] Alg/Sr hydrogel passed the direct contact test with fibroblast cells (L-929) without cell population reduction.[35] RADMSCs isolated from Rabbit Adipose tissue. The result of this test was grade zero which indicates no detectable zone found around or under specimen. Any zone extending more than 0.33 cm can count it as grade 4 or severe respond to the cells.

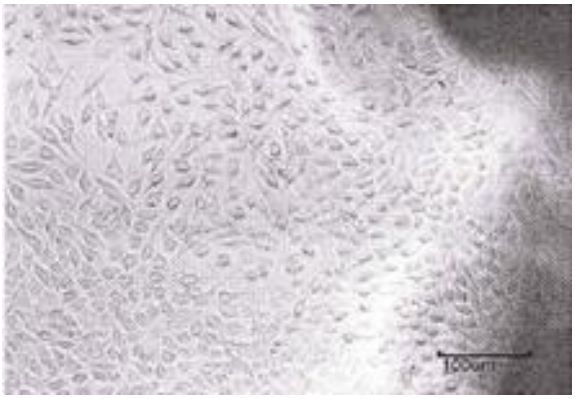

Fig 12: No cytotoxic reactivity to fibroblast cells (L-929) after 24 Hours of contact with Alg/Sr hydrogel.

Animal ethics and stem cell approval

This study was using MSCs which have been approved by the Institutional Committee for Stem Cell Research and Therapy (IC-SCRT: SCT/IC-SCTY/11/JAN 2013). Animal experiments were performed following the guidelines and recommendations of the Committee for the Purpose of Control and Supervision of Experiments on Animals, India (CPCSEA) and with the approval from Institutional Animal Ethics Committee (IAEC: B3112010VIII).

Cell surface characterization

Cell-surface immunophenotype for RADMSCs were positive for CD 90 and CD 105.

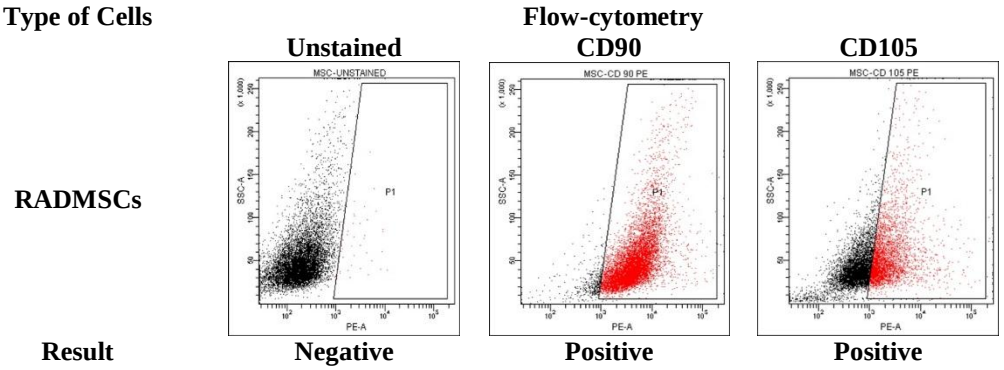

Fabrication of 3D tissue-engineered construct - Cell titer test

RADMSCs were cultured in the hydrogel for proliferation assay and compared with growth of cells in the normal condition in 48 wells plate. The same numbers of cells used for in *vivo* condition has been used in the cell proliferation assay too. Cells were counted with hemocytometer and confirmed by scepter cell counter 1.2* 10^5 Cells[36],[37] for encapsulation within the 3D hydrogel where cells proliferated and remained viable. In the day 3 and 7 there were significant increasing in cell number compare to the test on day 3 and 7. Proliferation assay of RADMSCs revealed better growth of cells in 3 D Alg/Sr hydrogel increasing in number compared to cells alone as control . Cell growth in 3D is better than 2D culture conditions (Chen et al., 2015).

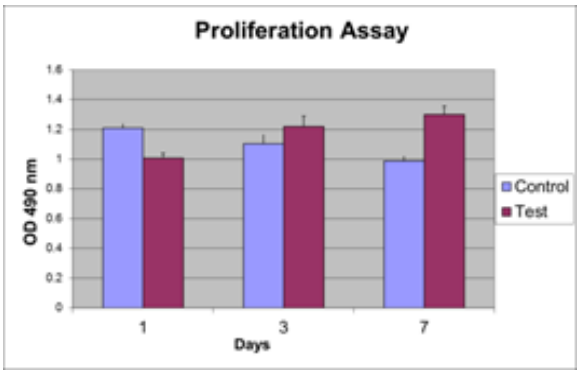

Fig 13: Cell number increased with 7 days of 3D culture. Number of cells decreased in the control (cells alone).

Encapsulation of MSCs in 3D cylindrical gel block

In this study the cell number used was 1.2*10^5 and cells were visible under the inverted microscope. 3D design of hydrogel encapsulated cell revealed very nicely pattern of cell expansion in the hydrogel. RADMSCs were cultured in 3D cylindrical Alg/Sr hydrogel blocks for its viability test. Spindle shaped cells ADMSCs proliferated and expanded in 3D culture visible by light microscopy.

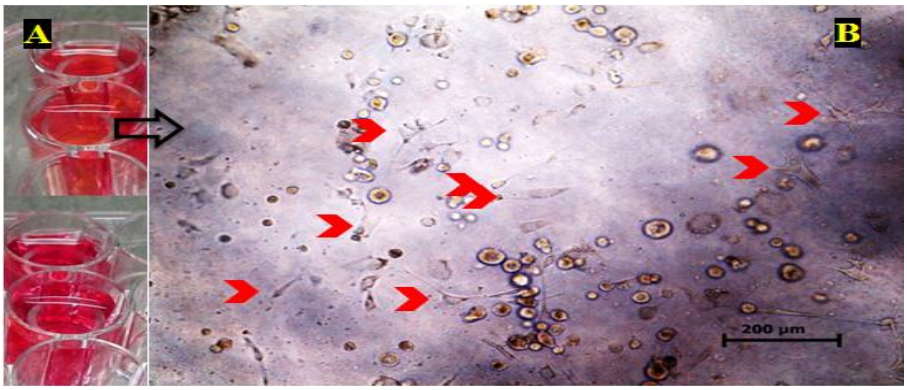

Fig 14: Light micrograph of RADMSCs encapsulated in 3 D cylindrical Alg/Sr hydrogel block. Arrows indicates RADMSCs in side Alg/Sr hydrogel (B).

Actin staining

Actin/DAPI staining was done to depict the presence of cells within the depth of hydrogel which was revealed by confocal microscopy by the blue stained nucleus of clustered cells. Alg/Sr hydrogel encapsulated the cells and provided a habitat for them to multiple and expand profusely retaining their spindle shape visible in the environment friendly 3D hydrogel block. Illustration of actin by confocal microscopy revealed nucleus of clustered cells at different depths of the hydrogel. Cells were alive and in 3D z-stack mode thickness of cell population could be captured.

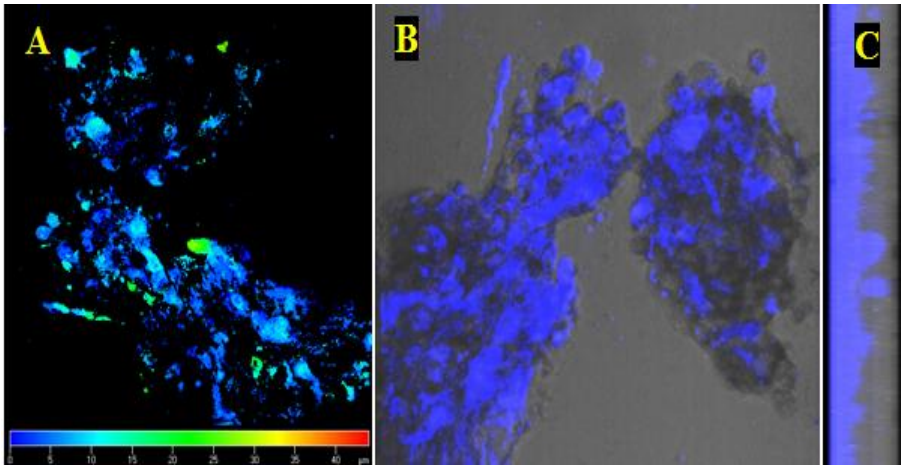

Fig 15: Confocal Micrographs of cluster of RADMSCs encapsulated in Alg/Sr hydrogel (A, B) DAPI Staining. Actin filament (green) and nucleus (blue). Depth of Alg/Sr Hydrogel - 3D image (C).

Cell viability assay

Live – dead assay was done due to understand the viability of cells within the depth of hydrogel. Green cluster of cells shows viable cells in the depth of hydrogel. In 3D micrograph thickness and cluster of cell is visible. Live-Dead assay of cells within Alg/Sr hydrogel revealed healthy encapsulated cells in the hydrogel block. Green cluster of cells were visualized by confocal imaging and in 3D z-stack mode imaging, cells were visualized in the center of the hydrogel block. This indicated eco-friendly environment of Alg/Sr hydrogel for cell growth, expansion, attachment and differentiation.

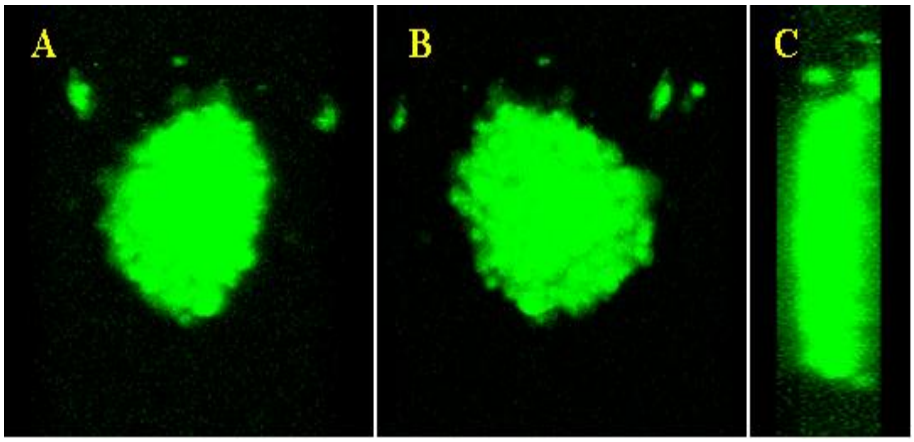

Fig 16: Confocal Micrographs of cluster of RADMSCs encapsulated in Alg/Sr hydrogel, (A, B) - Acridine Orange (Green- live cell stain) and ethidium bromide (Red- dead cell stain). Depth of section and orientation of cells within the hydrogel (C).

***In vivo* Experiments - Rabbit Intervertebral disc (IVD) defect model**

According to the measurement on rabbit IVD, distance between outer layers of IVD to center of NP is equal to 3.89 mm. It means that for puncturing and insertion of hydrogel needle the distance to be covered by needle is 3.89 mm and further insertion of the needle more than 5 mm will prick the spinal cord and ultimately the rabbit will paralyze. During surgery, tip of the needle is marked for a maximum of 4 mm prior to insertion into the intervertebral disc.[24]

Rabbit Implantation experiment

By setting up all requirements for the first surgery, rabbit undergoes anesthesia for developing the NP-IVD degenerative model by opening up from the left mid dorsolateral side. Pelvic bone can be used as a land mark for counting vertebrae from L7 to L1. The physical

injury with the needle is done on the NP of the IVD mainly on L4/L5 or L5/L6 to create the NP-IVD model. Thereafter post one month of physical injury, rabbit was taken for X-ray radiography to confirm NP degeneration of L5/L6 region compared to the control animal.

Development of Rabbit IVD Model and Resurgery

After every surgery rabbit was checked for any pain and behavioral changes.[38] Here, the rabbits were able to curl and walk which indicated that surgery was fine and there was no harm to spinal cord and only the intervertebral disc was targeted. In this study, no animals were paralyzed due to the expertise surgical skill.

Radiography of Re-surgery and injection of bare Alg-Sr hydrogel/cell combination

X-Ray radiographs revealed degeneration in the L5/L6 in the Rabbit NP-IVD model (sham), Interestingly, regeneration of the injured NP of the intervertebral disc of Alg/Sr-cells Group and Alg/Sr Group was evident from the radiograph after a period of three and six months respectively. Alg/Sr hydrogel alone and with cells were injected into the injured NP, post one month of degeneration for a period of one, three and six months respectively. Thereafter radiography evaluations indicated degeneration still persisted in the L5/L6 sham group while considerable regeneration of NP after 3 months in the Alg/Sr alone group and Alg/Sr in cooperated with cells were observed.

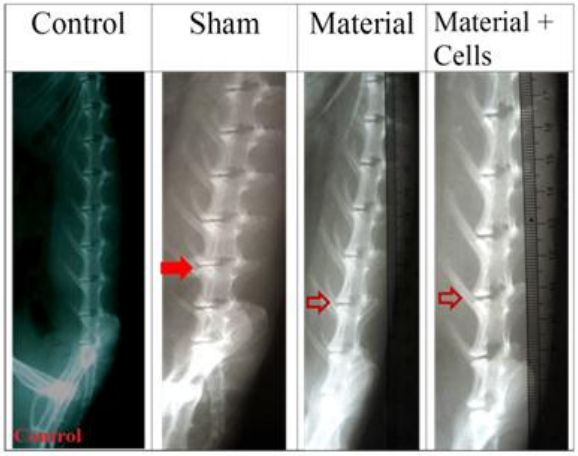

Fig 17: Radiographs of Rabbit lumbar region gap between 2 vertebrae in Material cells Group is more than sham after a period of 3 months.

Rabbit gait and behavior – post surgery and post implantation

Post-surgery of NP degeneration and again re-surgery thereafter for introducing the hydrogel with and without cells, experimental rabbits showed normal gait and behavior where they are able to walk and feed and drink ad libitum. This indicated that damage was restricted to the NP area of the IVD alone and the spinal cord is uninjured. There was neither inflammation nor necrosis and healing was uneventful.

Fig 18: Rabbit behavior – gait and movement (1) post-physical injury of NP degeneration in developing the IVD model (A, B); (2) injection of Alg/Sr with cells (C, D), one month post NP injury.

Post implanted evaluations in Rabbit IVD model

MRI imaging also confirmed increase of disc height index (DHI) in Alg/Sr and Alg/Sr combined cell group by T2 MRI system.[39],[40]

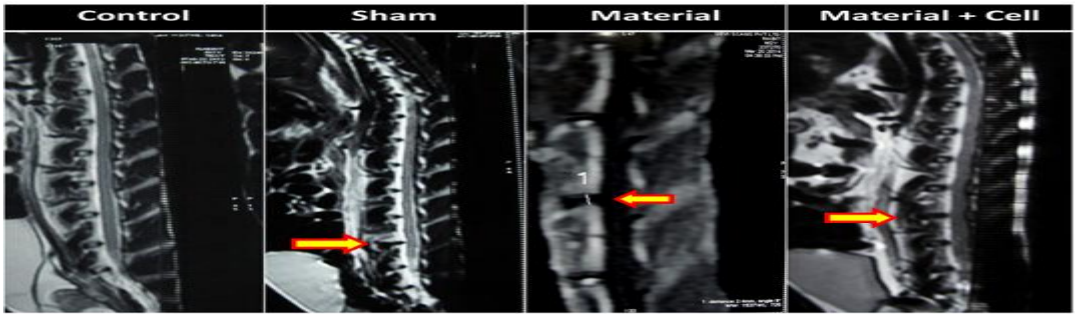

Fig 19: MRI images showed good regeneration at NP-IVD defect site in Material+ cells and Material Groups compared to Sham.

Histological evaluation

Light micrographs indicated that in sham group total degeneration was observed after one month. After 3 months, regeneration was observed in the material Group. By 6 months, regeneration was observed in the damaged NP-IVD. Regeneration in material-cell Group was high in 3 months comparable with the control Group. Histology evaluation revealed NP regeneration on Alg/Sr and cell –Alg/Sr groups. In the 6 months Alg/Sr group there was significant regeneration compared to sham 6 months. In 3 months cell/Alg group, regeneration rate was more than 3 months Alg/Sr and sham.

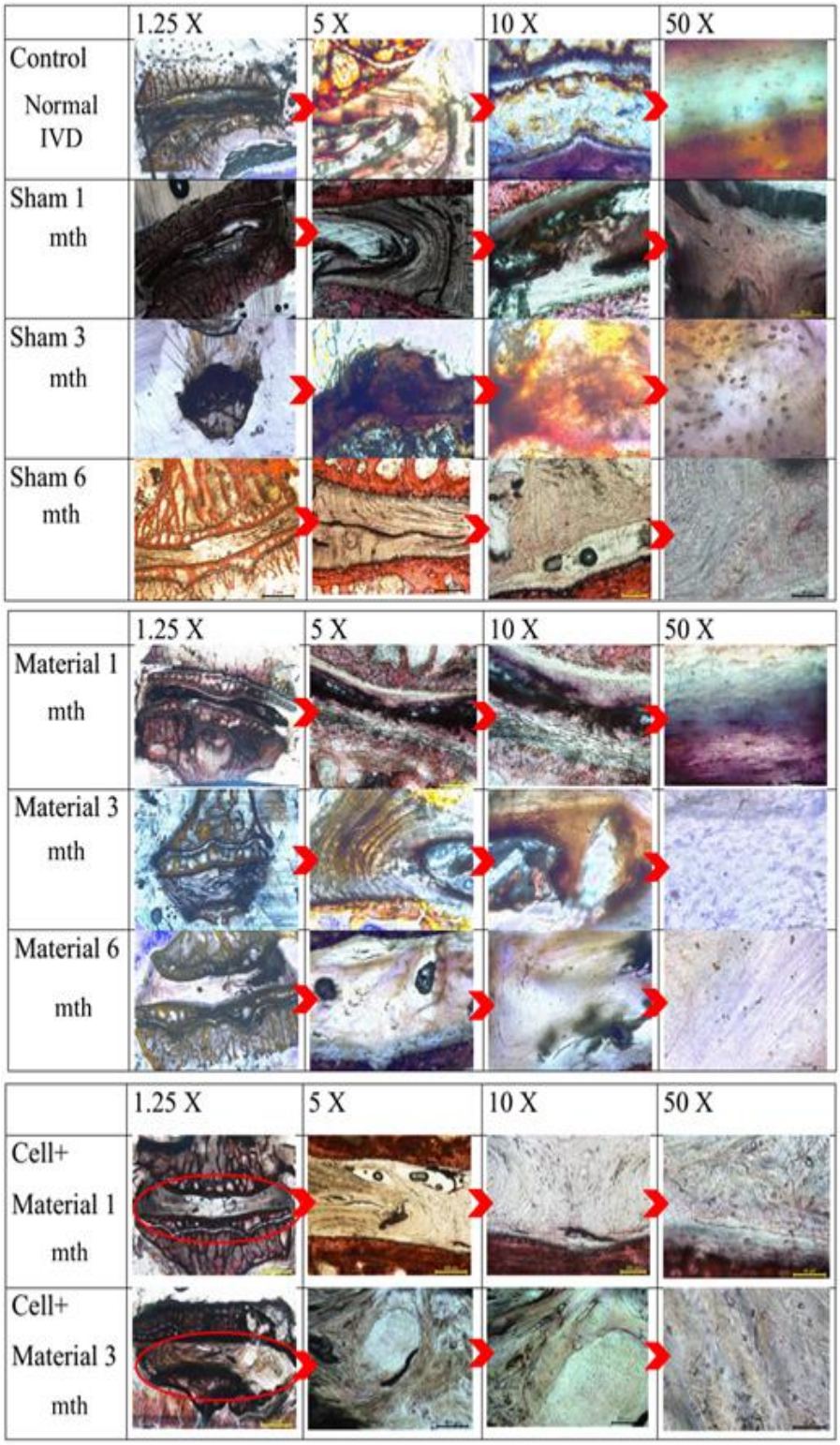

Fig 20: Light Micrographs of rabbit lumbar NP-IVDs of Control, sham, material and cells with material Groups at time intervals of one, three and six months.

Histomorphometric evaluation

Histomorphometry was done according to the area of regeneration at the NP-IVD defect site. Many reports explained the production of extra cellular matrix and COL II which indicates NP is under the healing process rather than evaluate the disc height (Fontana et al., 2014; H et al., 2010; Li et al., 2014). After expression of the extra cellular matrix by cells, the environment of NP must be stable and stiff to sustain the disc height for a period of time. Normally the disc height increases temporarily but continuation of healing process is the most challenging part of IVD regeneration.

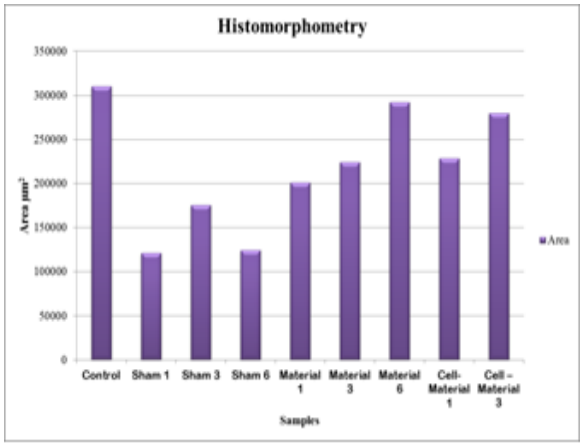

Fig 21: Regeneration of intervertebral disc by measuring total area of space between two vertebrae.

Disc Grading Evaluation

In this study, NP regeneration was evident by histomorphometric analysis and in turn by the disc height index over a period of time. Histology was evaluated with Disc Height Grading Index-one month sham as grade 5 (total degeneration) while in sham 3 and 6 months there was minimum regeneration of the degenerated tissue initiating healing (Roberts et al., 1997; Wilke et al., 2006). Alg-Sr group after 3 months showed good progress of healing. However, in the cell-Alg/Sr group, good regeneration of intervertebral disc was observed in the first month itself and thereafter 3 months it was more than 90%. Alg-Sr & cell combination product healing at 3 months is comparable to bare Alg-Sr hydrogel at 6 months. Hence, "Alg-Sr & cell combination product" definitely helped in enhancing the healing of the damaged NP and increasing the disc height index.

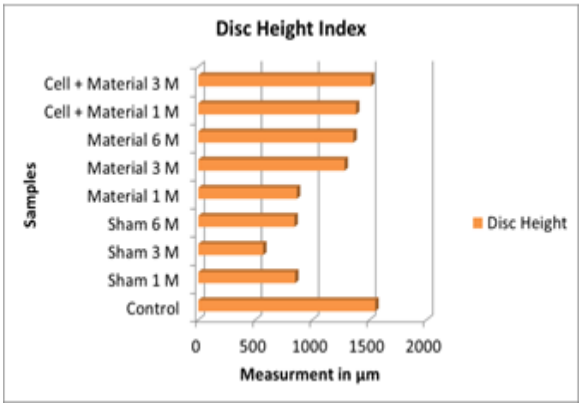

Fig 22: Disc Height Index of the regenerated disc in Rabbit NP-IVD defect model in – Control, Sham, Material, Cells with Material Groups at different period of one , three and six months.

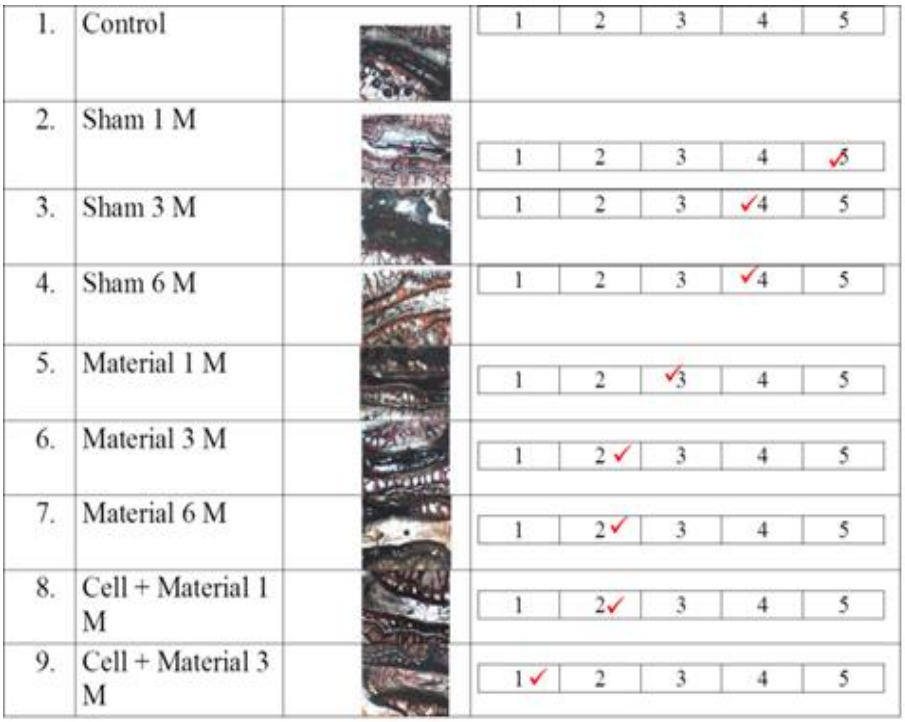

Fig 23: Disc Grading remarks which was done blindly with a pathologist which sample name was unknown.

The distribution of polymer in the gel beads varied greatly depending on both the concentration and type of divalent ions used for gelling purposes. It has been shown that low concentrations of ions in the gelling solution will give the alginate more time to diffuse to the bead surface as the driving force of ions toward the gelling zone is reduced. The osmotic pressure in an alginate gel is proportional to the alginate concentration, while the number of cross-links is proportional to the concentration in the second power. By increasing the alginate concentration at the surface and increasing the cross-link density using barium or strontium ions in combination with an alginate with a high G content, the stability of beads should be greatly increased. High cell numbers like $2*10^6$, $3.3*10^6$ can easily lead to cell clusters and ultimately to apoptosis. Researchers could reduce the speed of degeneration but production of extra cellular matrix was less.[41],[42] Many researchers preferred to isolate NP cells rather than adult stem cells. The disadvantage of using NP cells is that they are already under pressure and these cells are exhausted and under the influence of different types of internal cytokines to form cell clusters.[24],[43],[44] The advantage of RDAMSCs is that they are fresh cells and encourage co-culture systems under hypoxy condition when they are injected into the nucleus pulposus. The newly arrived cells in the NP are induced to differentiate into NP-like cells influenced by the host NP cells for which growth factors are not required.

CONCLUSION

Compared to other studies, this preclinical study mainly focused on the stiffness and load bearing of hydrogel to permit cells to proliferate, expand and provide extra cellular matrix to increase the disc height by regeneration of the defected disc and revert to normal function. Further study in a larger animal NP-IVD model is warranted prior to clinical trials, The Alg/Sr hydrogel scaffold is a potential candidate for tissue engineered nucleus pulposus. In the clinical perspective, "Alg-Sr & cell combination product" may be an interim relief to improve the quality of life of the younger generation affected by low back pain. Though results from all animal models are impressive, questions remain unanswered - as to whether a quadruped disc with its very different load can serve as an adequate model for biped disc repair. Again, can an acute disc model created in all animal models be a surrogate for chronic degenerated disc normally encountered in patients (Yoshikawa et al., 2010). There's a long way to go before an optimal scaffold for NP-IVD repair is identified and a combinatorial application of adult stem cells and injectable hydrogels will be advantageous in NP tissue engineering. Besides conservative and surgical treatments (removal of disc and vertebra fusion), cell therapy foresees the possibility of regenerating the damaged NP where cells can proliferate *in vitro* and re-implanted to alleviate the pain and further prolong the damage to sustain quality of life. Hence, the prospect of cell-based Nucleus Pulposus (NP) tissue-engineering strategy has become attractive and relevant in Regenerative Medicine.

ACKNOWLEDGEMENTS

The Authors gratefully acknowledge The Director SCTIMST and The Head, BMT, SCTIMST, for the facilities to carry out this work; Centre for International Co-operation in Science (CICS) Fellowship for Mir Mahmoud Mortazavi R; Funding support from Kerala State Council for Science, Technology & Environment (KSCSTE), Trivandrum; and Dr. Suresh S Pillai, Senior Consultant, Orthopaedics & Spine Surgeon, Aster MIMS, Calicut - is also gratefully acknowledged in this IVD research programme.

REFERENCES

1. B. G. M. van Dijk, E. Potier, and K. Ito, "Long-term culture of bovine nucleus pulposus explants in a native environment," *Spine J.*, Apr. 2013; 13(4): 454–463.
2. S. C. W. Chan, A. Bürki, H. M. Bonél, L. M. Benneker, and B. Gantenbein-Ritter, "Papain-induced in vitro disc degeneration model for the study of injectable nucleus pulposus therapy," *Spine J. Off. J. North Am. Spine Soc.*, Mar. 2013; 13(3): 273–283.
3. E. Mavrogonatou, K. Papadimitriou, J. P. Urban, V. Papadopoulos, and D. Kletsas, "Deficiency in the α1 subunit of Na+/K+-ATPase enhances the anti-proliferative effect of high osmolality in nucleus pulposus intervertebral disc cells," *J. Cell. Physiol.*, Dec. 2015; 230(12): 3037–3048.
4. L. Dang and Z. Liu, "A review of current treatment for lumbar disc herniation in children and adolescents," *Eur. Spine J.*, Feb. 2010; 19(2): 205–214.
5. C. R. Good, J. D. Auerbach, P. T. O'Leary, and T. C. Schuler, "Adult spine deformity," *Curr. Rev. Musculoskelet. Med.*, Oct. 2011; 4(4): 159–167.
6. A. T. Francisco, P. Y. Hwang, C. G. Jeong, L. Jing, J. Chen, and L. A. Setton, "Photocrosslinkable laminin-functionalized polyethylene glycol hydrogel for intervertebral disc regeneration," *Acta Biomater.*, Mar. 2014; 10(3): 1102–1111.
7. T. Kadow, G. Sowa, N. Vo, and J. D. Kang, "Molecular Basis of Intervertebral Disc Degeneration and Herniations: What Are the Important Translational Questions?," *Clin. Orthop.*, Jun. 2015; 473(6): 1903–1912.
8. K. Hemmrich *et al.*, "Autologous in vivo adipose tissue engineering in hyaluronan-based gels--a pilot study," *J. Surg. Res.*, Jan. 2008; 144(1): 82–88.
9. G. Pattappa, Z. Li, M. Peroglio, N. Wismer, M. Alini, and S. Grad, "Diversity of intervertebral disc cells: phenotype and function," *J. Anat.*, Dec. 2012; 221(6): 480–496.
10. J. A. Hunt, R. Chen, T. van Veen, and N. Bryan, "Hydrogels for tissue engineering and regenerative medicine," *J. Mater. Chem. B.*, Jul. 2014; 2(33): 5319–5338.

11. J. Kopecek, "Hydrogel biomaterials: a smart future?," *Biomaterials*, Dec. 2007; 28(34): 5185–5192.
12. J. L. Bron, L. A. Vonk, T. H. Smit, and G. H. Koenderink, "Engineering alginate for intervertebral disc repair," *J. Mech. Behav. Biomed. Mater*, Oct. 2011; 4(7): 1196–1205.
13. J. A. Rowley, G. Madlambayan, and D. J. Mooney, "Alginate hydrogels as synthetic extracellular matrix materials," *Biomaterials*, Jan. 1999; 20(1) 45–53.
14. C.-Y. Chen, C.-J. Ke, K.-C. Yen, H.-C. Hsieh, J.-S. Sun, and F.-H. Lin, "3D Porous Calcium-Alginate Scaffolds Cell Culture System Improved Human Osteoblast Cell Clusters for Cell Therapy," *Theranostics*, Mar. 2015; 5(6): 643–655.
15. A. I. Chou and S. B. Nicoll, "Characterization of photocrosslinked alginate hydrogels for nucleus pulposus cell encapsulation," *J. Biomed. Mater. Res. A*, Oct. 2009; 91(1): 187–194.
16. A. D. Augst, H. J. Kong, and D. J. Mooney, "Alginate hydrogels as biomaterials," *Macromol. Biosci*, Aug. 2006; 6(8): 623–633.
17. E. M. Ahmed, "Hydrogel: Preparation, characterization, and applications: A review," *J. Adv. Res.*, Mar. 2015; 6(2): 105–121.
18. B. P. Chan and K. W. Leong, "Scaffolding in tissue engineering: general approaches and tissue-specific considerations," *Eur. Spine J.*, Dec. 2008; 17(4): 467–479.
19. S. N. Pawar and K. J. Edgar, "Alginate derivatization: A review of chemistry, properties and applications," *Biomaterials*, Apr. 2012; 33(11): 3279–3305.
20. O. Bruyere *et al.*, "Effects of strontium ranelate on spinal osteoarthritis progression," *Ann. Rheum. Dis.*, Mar. 2008; 67(3): 335–339.
21. W. J. C. M. Marijnissen *et al.*, "Alginate as a chondrocyte-delivery substance in combination with a non-woven scaffold for cartilage tissue engineering," *Biomaterials*, Mar. 2002; 23(6): 1511–1517.
22. S. H. Hong *et al.*, "STAPLE: Stable Alginate Gel Prepared by Linkage Exchange from Ionic to Covalent Bonds," *Adv. Healthc. Mater*, Jan. 2016; 5(1): 75–79.
23. Y. A. Mørch, I. Donati, B. L. Strand, and G. Skjåk-Braek, "Effect of Ca2+, Ba2+, and Sr2+ on alginate microbeads," *Biomacromolecules*, May 2006; 7(5): 1471–1480.
24. M. H. Kong, D. H. Do, M. Miyazaki, F. Wei, S.-H. Yoon, and J. C. Wang, "Rabbit Model for in vivo Study of Intervertebral Disc Degeneration and Regeneration," *J. Korean Neurosurg. Soc.*, Nov. 2008; 44(5): 327–333.
25. M. Alini *et al.*, "Are animal models useful for studying human disc disorders/degeneration?," *Eur. Spine J. Off. Publ. Eur. Spine Soc. Eur. Spinal Deform. Soc. Eur. Sect. Cerv. Spine Res. Soc.*, Jan. 2008; 17(1): 2–19.
26. C. Daly, P. Ghosh, G. Jenkin, D. Oehme, and T. Goldschlager, "A Review of Animal Models of Intervertebral Disc Degeneration: Pathophysiology, Regeneration, and Translation to the Clinic," *BioMed Res. Int.*, May 2016; e5952165.
27. J. B. Greenaway, G. D. Partlow, N. L. Gonsholt, and K. R. Fisher, "Anatomy of the lumbosacral spinal cord in rabbits," *J. Am. Anim. Hosp. Assoc.*, Feb. 2001; 37(1): 27–34.
28. M. B. Nair, G. Baranwal, P. Vijayan, K. S. Keyan, and R. Jayakumar, "Composite hydrogel of chitosan-poly(hydroxybutyrate-co-valerate) with chondroitin sulfate nanoparticles for nucleus pulposus tissue engineering," *Colloids Surf. B Biointerfaces*, Dec. 2015; 136: 84–92.
29. L. Li, L. Lu, and C. Zhou, "Notice of RetractionFabrication of Injectable PLLA/Alginate Hydrogel for Tissue Engineering," in *2011 5th International Conference on Bioinformatics and Biomedical Engineering*, 2011; 1–4.
30. L. Calderon, E. Collin, D. Velasco-Bayon, M. Murphy, D. O'Halloran, and A. Pandit, "Type II collagen-hyaluronan hydrogel--a step towards a scaffold for intervertebral disc tissue engineering," *Eur. Cell. Mater*, 2010; 20: 134–148.
31. J. Silva-Correia *et al.*, "Gellan gum-based hydrogels for intervertebral disc tissue-engineering applications," *J. Tissue Eng. Regen. Med.*, Jun. 2011; 5(6): e97-107.
32. W. E. Roorda, J. A. Bouwstra, M. A. de Vries, and H. E. Junginger, "Thermal analysis of water in p(HEMA) hydrogels," *Biomaterials*, Nov. 1988; 9(6): 494–499.
33. Z. Megeed, J. Cappello, and H. Ghandehari, "Thermal Analysis of Water in Silk−Elastinlike Hydrogels by Differential Scanning Calorimetry," *Biomacromolecules*, May, 2004; 5(3): 793–797.
34. M. Annunziata *et al.*, "In vitro biological response to a light-cured composite when used for cementation of composite inlays," *Dent. Mater. Off. Publ. Acad. Dent. Mater*, Dec. 2006; 22(12): 1081–1085.
35. K. G. Ozdemir, H. Yilmaz, and S. Yilmaz, "In vitro evaluation of cytotoxicity of soft lining materials on L929 cells by MTT assay," *J. Biomed. Mater. Res. B Appl. Biomater.*, Jul. 2009; 90(1): 82–86.
36. D. O. Halloran, S. Grad, M. Stoddart, P. Dockery, M. Alini, and A. S. Pandit, "An injectable cross-linked scaffold for nucleus pulposus regeneration," *Biomaterials*, Feb. 2008; 29(4): 438–447.
37. M. Peroglio *et al.*, "Injectable thermoreversible hyaluronan-based hydrogels for nucleus pulposus cell encapsulation," *Eur. Spine J. Off. Publ. Eur. Spine Soc. Eur. Spinal Deform. Soc. Eur. Sect. Cerv. Spine Res. Soc.*, Aug. 2012; 21(6): S839-849.
38. D. B. Morton and P. H. Griffiths, "Guidelines on the recognition of pain, distress and discomfort in experimental animals and an hypothesis for assessment," *Vet. Rec.*, Apr. 1985; 116(16): 431–436.

39. N. M. Menezes, M. L. Gray, J. R. Hartke, and D. Burstein, "T2 and T1rho MRI in articular cartilage systems," *Magn. Reson. Med.*, Mar. 2004; 51(3): 503–509.
40. E. C. Krueger, J. O. Perry, Y. Wu, and V. M. Haughton, "Changes in T2 relaxation times associated with maturation of the human intervertebral disk," *AJNR Am. J. Neuroradiol.*, Aug. 2007; 28(7): 1237–1241.
41. K. Chiba, G. B. Andersson, K. Masuda, and E. J. Thonar, "Metabolism of the extracellular matrix formed by intervertebral disc cells cultured in alginate," *Spine*, Dec. 1997; 22(24): 2885–2893.
42. J. Yu, "Elastic tissues of the intervertebral disc," *Biochem. Soc. Trans.*, Nov. 2002; 30(6): 848–852.
43. J. Melrose, S. M. Smith, C. B. Little, R. J. Moore, B. Vernon-Roberts, and R. D. Fraser, "Recent advances in annular pathobiology provide insights into rim-lesion mediated intervertebral disc degeneration and potential new approaches to annular repair strategies," *Eur. Spine J.*, Sep. 2008; 17(9): 1131–1148.
44. Z. Sun *et al.*, "Effect of perfluorotributylamine-enriched alginate on nucleus pulposus cell: Implications for intervertebral disc regeneration," *Biomaterials*, Mar. 2016; (82): 34–47.